Acta Cryst. (1999). B**55**, 363–374

Accurate charge densities in days — use of synchrotrons, image plates and very low temperatures

B. B. Iversen,[a]* F. K. Larsen,[a] A. A. Pinkerton,[b] A. Martin,[b] A. Darovsky[c] and P. A. Reynolds[d]

[a]*Department of Chemistry, University of Aarhus, DK-8000 Aarhus C, Denmark,* [b]*Department of Chemistry, University of Toledo, Toledo, OH 43606, USA,* [c]*National Synchrotron Light Source, Brookhaven National Laboratory, Upton, NY 11973, USA, and* [d]*Research School of Chemistry, Australian National University, Canberra, ACT 0200, Australia. E-mail: bo@kemi.aau.dk*

(*Received 1 April 1998; accepted 30 July 1998*)

Abstract

Extensive synchrotron (28 K) and conventional sealed-tube (9 K) X-ray diffraction data have been collected on tetrakis(dimethylphosphinodithioato-*S*,*S*′)thorium(IV), $[Th(S_2PMe_2)_4]$. The use of very low temperatures, well below those obtained with liquid-nitrogen cooling, is crucial for the accuracy of the data. This is due to minimization of temperature-dependent systematic errors such as TDS and anharmonicity, and extension and intensification of the data in reciprocal space. Comparison of structural parameters derived separately from the sealed-tube data and the synchrotron data shows good agreement. The synchrotron data are markedly superior when comparing refinement residuals, standard uncertainties (s.u.'s) of the data and s.u.'s of the derived parameters. However, the study suggests that there are still small uncorrected systematic errors in the data. The very large extent $[(\sin\theta/\lambda)_{max} = 1.77\ \text{Å}^{-1}]$ of the synchrotron data and the very low temperature at which they were collected makes it possible to separate anharmonic effects from electron-deformation effects even with only an X-ray data set at a single temperature. The electron density shows a large polarization of the outer Th core of *d*-type symmetry. This deformation is successfully modelled with contracted multipolar functions, which are only slightly correlated with anharmonic expansions in reciprocal space when using the full extent of the data. In the data collection more than a factor of 100 in speed is gained by use of image-plate area detectors at the synchrotron source compared with conventional sequential measurements. Thus accurate, very low temperature synchrotron-radiation diffraction data can now be measured within days, which makes electron-density studies of compounds beyond the first transition series more frequently within reach.

1. Introduction

Synchrotron radiation has the potential to enhance the accuracy of X-ray diffraction data, facilitating an improvement in derived electron densities (Coppens, 1992). This is primarily due to minimization of systematic errors such as absorption and extinction by the use of short-wavelength radiation and small crystal specimens. One serious problem at synchrotron sources has been adequate monitoring of the incident X-ray beam to correct for both its decay and for small short-time intensity variations. The pioneering synchrotron-radiation electron-density (ED) study was carried out at the CHESS synchrotron on $Cr(NH_3)_6Cr(CN)_6$ by Nielsen *et al.* (1986). This study showed that good single-crystal diffraction data could be collected at synchrotron sources. Considerable progress was reported by Kirfel & Eichhorn (1990), who used careful beam monitoring to measure data in sequential mode for Al_2O_3 and Cu_2O at HASYLAB. The data clearly revealed the advantage of the intense synchrotron beam, especially in the measurement of weak reflections. However, it was clear that sequential measurements on crystals of chemical complexity could never be routine at synchrotron sources due to beam-time limitations. Measuring time for typical small-molecule structures easily amounts to 1–2 months. Fortunately, advances in area-detector technology have occurred, making it possible to collect many reflections simultaneously.

However, in order to measure accurate diffraction data it is also imperative to measure at the lowest possible temperature (Larsen, 1995), and this produces further problems when using area detectors. In a series of papers we have shown that very significant improvements are gained in data accuracy when data are measured with helium cooling (∼10 K) compared to nitrogen cooling (∼100 K) (Figgis *et al.*, 1993; Chandler *et al.*, 1994; Iversen *et al.*, 1996, 1997). The improvements are due to minimization of temperature-dependent systematic errors such as TDS and anharmonicity. Even in fairly hard materials such as metallic magnesium the TDS contribution to the intensity is about 8% for medium-order data (0.7–0.8 Å^{-1}) at 125 K (Iversen *et al.*, 1995). Anharmonic motion can also be very significant at temperatures close to liquid-nitrogen temperature as observed, for example, in copper Tutton salt at 85 K (Figgis *et al.*, 1992). Since electron deformation and anharmonic motion are quite correlated it is clear that anharmonicity can be a serious systematic error in

studies focused on bonding (Restori & Schwarzenbach, 1996). In our previous very low temperature studies it was shown that when modelling 10 K diffraction data it is necessary to introduce electronic models of unprecedented flexibility to attain a satisfactory description of the data. This is in part because of the overall much smaller thermal motion, which allows a better resolution of bonding features. Furthermore, comparison with current theory revealed that for transition metal systems very accurate 10 K data contain information that cannot yet be obtained from theory.

Measurement of data at very low temperatures using an area detector is far from trivial. While most laboratories can routinely measure data with a nitrogen gas-stream flow, diffractometers using Displex helium refrigerators are still relatively rare (Larsen, 1995). The problem with an area detector is that it also detects the parasitic scattering from the vacuum cups of the Displex refrigerator. In sequential measurements this scattering can be removed by proper collimation. The parasitic scattering leads to intolerably large background intensities on the area detector. The problem was solved by A. Darovsky at beamline X3 at the NSLS by development of an antiscatter device which fits inside the vacuum cups of the Displex refrigerator (Darovsky *et al.*, 1994). The first area-detector ED data sets recorded at synchrotron sources were published by Bolotovsky, Darovsky *et al.* (1995) using this device. In just two days, full data sets were measured with 0.394 Å radiation at 50 K on the same compound as the initial CHESS study, $Cr(NH_3)_6Cr(CN)_6$, and at *ca* 100 K on sodium nitroprusside. The study showed that an accuracy comparable to conventional sequential data was achievable, and experimental deformation maps clearly showed details such as nitrogen lone-pair density. However, these data were still only preliminary since important systematic errors had still not been removed. One of these was only recently discovered and concerns the beam path of the X-ray in the image plate (Zaleski *et al.*, 1998).

Recently Koritzansky *et al.* (1998) reported a synchrotron ED study at 100 K on a simple organic molecule using a CCD detector. These data were measured in just a single day, but were not very extended in reciprocal space [$(\sin\theta/\lambda)_{max} = 1.12$ Å^{-1}]. Analysis of the derived ED showed that good internal consistency for related electronic properties could be achieved. However, since this study was not at very low temperatures the data were prone to the systematic errors discussed above. While liquid-nitrogen studies with CCD detectors are precise, further lowering of the temperature is generally crucial for accuracy due to the relative softness of most chemically relevant materials. This is especially important for studies of heavy-metal compounds where the need for accuracy is more critical than in studies of organic molecules (Stevens & Coppens, 1976). Throughout the paper we will use the term accurate in the statistical sense, that is accuracy as opposed to precision. It is expected that there will be a considerable growth in the field of experimental ED studies due to the availability of fast area detectors. It is therefore important at this point to examine the accuracy of such data.

The structure of $[Th(S_2PMe_2)_4]$, Fig. 1, is attractive for an accurate study by X-ray diffraction because it contains a Th—S bond likely to be a real test for theoretical studies. Experimentally, the study of heavy elements demands more accurate data since the heavier the element, the smaller the fraction of scattering by the valence electrons relative to the core contribution. The study has some hope of success since the crystal structure is unusually simple and symmetrical for such a heavy-metal complex. It involves only six non-H and six H unique atoms, a neutral molecule of D_2 symmetry in a crystal of tetragonal symmetry (Pinkerton *et al.*, 1981). Crucially one half of the reflections ($h + k + l$ odd) contain *no* contribution from the spherical component of the electron-rich thorium core. Thus these reflections may provide good data concerning the ligand electron distribution, unaffected by the heavy-metal core. The previous study was directed towards structure determination, being based on room-temperature data and of low resolution, but it gave an encouraging agreement factor $R(F)$ of 0.03. Our subsequent unpublished studies at higher resolution at both room temperature and liquid-nitrogen temperature gave improved agreement, and caused us to commence the study described in this paper. In the present case we have obtained data using both a conventional X-ray source and a synchrotron. The wavelengths used are lower than Mo $K\alpha$, since for

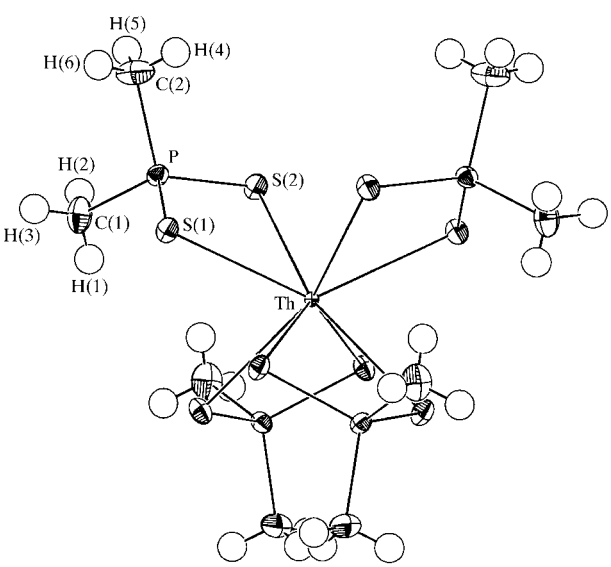

Fig. 1. An *ORTEP* (Burnett & Johnson, 1996) drawing of $[Th(S_2PMe_2)_4]$ showing 90% displacement ellipsoids and the atom-numbering scheme based on the LO synchrotron data set.

Table 1. *Experimental details*

	Sealed-tube Ag $K\alpha$ data	LO synchrotron data	HO synchrotron data
Wavelength (Å)	0.5603	0.394 (2)	0.394 (2)
Temperature (K)	9 (1)	28 (5)	28 (5)
Crystal form	Octahedron, 0.076 mm face-to-face	Octahedron, 0.076 mm face-to-face, corner off	Octahedron, 0.076 mm face-to-face, corner off
Chemical formula	$[Th(C_2H_6PS_2)_4]$	$[Th(C_2H_6PS_2)_4]$	$[Th(C_2H_6PS_2)_4]$
Chemical formula weight	732.7	732.7	732.7
$F(000)$	694.7	698.9	698.9
Cell setting	Tetragonal	Tetragonal	Tetragonal
Space group	$P4_22_12$	$P4_22_12$	$P4_22_12$
a (Å)	10.386 (1)	10.420 (4)	10.420 (4)
c (Å)	11.742 (2)	11.784 (8)	11.784 (8)
V (Å^3)	1266.6 (4)	1279 (1)	1279 (1)
Z	2	2	2
D_x (Mg m^{-3})	1.92	1.90	1.90
μ (mm^{-1})	5.35	2.23	2.23
T_{min}	0.42	0.72	0.72
T_{max}	0.49	0.76	0.76
θ range (°)	0–23, 30–32	0–22	5.5–43.9
Oscillation intervals		$2\theta = 0°$, 8° rotation, 2° overlap, 10 min exposure, $0 < \varphi < 270°$, 57 plates; 20° rotation, 17° overlap, 10 min exposure, $0 < \varphi < 132°$, 45 plates	$2\theta = 50°$, 5° rotation, 2° overlap, 15 min exposure, $0 < \varphi < 92°$ and $270 < \varphi < 362°$, 60 plates
Range of h, k, l	$-19 \rightarrow h \rightarrow 19$ $-6 \rightarrow k \rightarrow 19$ $-22 \rightarrow l \rightarrow 22$	$-35 \rightarrow h \rightarrow 29$ $-29 \rightarrow k \rightarrow 29$ $-18 \rightarrow l \rightarrow 41$	$-35 \rightarrow h \rightarrow 29$ $-29 \rightarrow k \rightarrow 29$ $-18 \rightarrow l \rightarrow 41$
No. of measured reflections	5826	81 185	38 969
$R1$†, $R2$‡, wR§ (all data)	0.028, 0.029, 0.037	0.050, 0.081, 46.87	0.017, 0.044, 0.174
(N_{data}, N_{means})	(5686, 2395)	(73 071, 3954)	(17 875, 6060)
$\sin\theta/\lambda < 0.5$ Å^{-1}	0.023, 0.028, 0.026	0.034, 0.055, 0.082	0.030, 0.136, 0.186
(N_{data}, N_{means})	(1924, 644)	(16 913, 657)	(608, 182)
No. of independent reflections (N_{obs})	2529	3677	12 671
N_{par}	137	151	105
Goodness-of-fit on F^2	1.14	0.83	1.89
$R[F^2 > 3\sigma(F^2)]$	0.022	0.011	0.030
$R(F^2)$ (all data)	0.033	0.014	0.042
$wR(F^2)$ (all data)	0.055	0.023	0.061

† $R1 = \sum |I - I_{mean}| / \sum |I|$. ‡ $R2 = [\sum (I - I_{mean})^2 / \sum I^2]^{1/2}$. § $wR = [\sum w(I - I_{mean})^2 / \sum wI^2]^{1/2}$.

this thorium-containing compound we need to minimize both absorption corrections and anomalous-dispersion effects more urgently than for lighter metals.

Here we present details of the data collections and data reductions. Furthermore, we show that the large extent of the data allows separation of anharmonic effects from electron-deformation effects with the use of only a single-temperature X-ray data set. Restori & Schwarzenbach (1996) have shown that for less extensive data sets these effects are not separable without the use of independent neutron parameters or X-ray data measured at several temperatures. Finally, we examine the structural parameters obtained from the refinements in order to learn about remaining systematic errors in the data. In a companion paper (Iversen *et al.*, 1998) we use the refined ED model to characterize the chemical bonding in actinide complexes and compare the results with high-quality *ab initio* calculations.

2. Experimental

2.1. *Conventional sealed-tube X-ray diffraction data collection*

The crystals were prepared by the method of Pinkerton *et al.* (1981). A small octahedrally shaped colourless crystal was encapsulated in a Lindemann glass capillary, fastened to the wall with vacuum grease. This was fitted to the triply beryllium-shielded cold finger of a type 202 Displex closed-cycle refrigerator mounted on a Huber type 512 four-circle diffractometer at the University of Aarhus (Henriksen *et al.*, 1986), and cooled to 9 (1) K over a period of 13 h. Ag $K\alpha$ radiation was used to minimize absorption. Cell dimensions were obtained by refining the setting angles of 44 well centred reflections in the range $30 < 2\theta < 50°$. Data were collected using $\omega/2\theta$ scans for three weeks, monitoring the intensity of four intense reflections every 50

measurements and the orientation matrix daily. The standard intensities all decreased uniformly and linearly with time, until at the end a loss of 20% of the initial intensity had occurred, resulting in a limited data set. A hemisphere of data was collected for $2\theta < 20^\circ$ and a quadrant (twice a unique set) for $20 < 2\theta < 46^\circ$ and $60 < 2\theta < 64^\circ$. The data are thus complete for $\sin\theta/\lambda < 0.697$ Å^{-1} with a shell $0.892 < \sin\theta/\lambda < 0.947$ Å^{-1}. Further experimental details are given in Table 1. Integrated intensities were obtained using the profile-analysis program *COLL5N* (Lehmann & Larsen, 1974), which is based on the minimization of $\sigma(I)/I$. The data were rescaled in intensity using the uniformly and linearly decreasing standard intensities, and corrected for absorption by numerical integration using a 512–point Gaussian grid with *DATAP* (Coppens, 1974). The contribution from the three beryllium cups was included in the absorption correction, but the contribution from the glass capillary was neglected. The data were averaged using *SORTAV* (Blessing, 1989).

2.2. *Synchrotron X-ray diffraction data collection*

An octahedral {011} crystal, with one corner missing to expose $(\bar{1}\bar{1}0)$, was mounted using the minimum quantity of epoxy glue on a few strands of thermally conducting carbon fibre. To establish good thermal conduction the fibres were then glued to a copper wire which was itself soldered to a brass pin directly mounted on the cold finger of a type 201 Displex refrigerator fitted with an anti-scattering device for image-plate measurements (Darovsky *et al.*, 1994). Temperature calibration established an absolute crystal temperature of 28 (5) K, although the stability during the three days of measurements was better than 1 K.

The data were measured at the X3A1 SUNY beamline of the NSLS at Brookhaven National Laboratory, which is of fixed wavelength and equipped with a Huber type 511 four-circle diffractometer. The wavelength of 0.394 (2) Å was obtained with an Si(200) double-crystal monochromator (Darovsky *et al.*, 1995). The data were recorded on 200 × 250 mm Fuji image plates mounted 155 mm from the sample on the 2θ arm of the diffractometer, and scanned off-line on a Fuji BAS2000 scanner (pixel size 0.1 × 0.1 mm, dynamic range 10^4). The data were recorded as two sets — hereafter known as low-order (LO) and high-order (HO) data sets — in which the θ arm was set with $2\theta = 0$ and 50°, respectively. Owing to beam-time limitations only one crystal setting in the cryo-refrigerator was used, and thus a blind region close to the rotation axis exists within the data. Nevertheless, owing to the relatively high space-group symmetry, an almost complete unique set of reflections was measured. The data were measured using φ oscillations but the orientation matrix was determined by use of a scintillation counter and normal four-circle methods. The standard uncertainties given in Table 1 for the synchrotron unit cell are the least-squares values obtained using a nominal wavelength of 0.394 Å. The two unit cells in Table 1 are identical if we assume the actual wavelength was 0.395 Å. In all least-squares refinements discussed below we have used the more accurate cell obtained from the sealed-tube measurements. ω scans showed a full width at half-maximum (FWHM) in the reflection profiles of 0.5° at low temperatures but only 0.1° at room temperature. This effect is reversible. It may be due to vibrations from the Displex compressor, which indeed in later studies have been shown to cause a peak broadening for crystals mounted on very thin carbon fibres not having adequate base support (Schultz, 1998). However, the absence of extinction at low temperatures (see below) suggests a possible, and unusual, real increase in crystal mosaicity. In some oscillation ranges low-angle reflections were saturated, and were remeasured and scanned at lower sensitivity to avoid saturation. Further experimental details are given in Table 1.

The intensities were indexed and integrated using the seed-skewness integration method with *IPMS* and *HIPPO* (Bolotovsky, White *et al.*, 1995). This method has been shown to extract weak intensities well (Bolotovsky & Coppens, 1997; Darovsky & Kezerashvili, 1997). Only fully recorded reflections having peak masks entirely inside the 3 × 3 mm^2 integration boxes were used, the minimum distance to neighbouring peaks was set at 1 mm and peaks closer than 0.25° to the edge of the oscillation interval were discarded. The data were corrected for Lorentz and polarization effects (92% incident-beam polarization; Darovsky, 1995) by the *HIPPO* program, and for non-normal beam incidence of the X-rays into the image plate using local software (Iversen, 1997). The latter correction was performed because it has recently been shown that most of the X-rays are transmitted through the image plates (Zaleski *et al.*, 1998). The intensities therefore have to be corrected for the actual beam path through the plates, which is dependent on the incident angle. The correction can be up to a factor two between high- and low-order intensities, and may also be important for CCDs. The data were corrected for absorption using the program *ABSORB* (DeTitta, 1985) using the measured crystal morphology. The linear absorption coefficient at 0.394 Å was calculated using another program called *ABSORB* (Brennan & Cowan, 1992). The data were subsequently averaged with *SORTAV* (Blessing, 1989), rejecting statistical outliers in multiple measurements (3.5% of LO and 1.6% of HO measured data). The s.u.'s calculated by *SORTAV* are based on the variance of the intensities of the unique data, which gives the s.u. of the sampled population. In some studies this value is divided by $(N_{\rm equivalent})^{1/2}$ to obtain the s.u. on the sample mean. This assumes that the errors are truly random and uncorrelated, which is almost certainly not fulfilled by the present image-plate data. We have therefore

Table 2. *Observed positional (S, P × 10^5, C × 10^4, H × 10^3) and harmonic displacement parameters (× 10^4 pm^2)*

The first line for each entry gives the values obtained from the sealed-tube data, the second line gives the values obtained from the LO synchrotron data and the third line gives the values obtained from the HO synchrotron data.

	x	y	z	U^{11}	U^{22}	U^{33}	U^{12}	U^{13}	U^{23}
Th	0	0	0	43 (2)	43	44 (1)	1 (1)	0	0
				23 (2)	23	26 (1)	1 (1)		
				24 (1)	24	25 (1)	1 (1)		
S(1)	−8771 (9)	24144 (9)	9888 (8)	51 (4)	59 (4)	61 (4)	6 (3)	−13 (3)	−5 (3)
	−8773 (3)	24137 (3)	9911 (3)	54 (1)	62 (1)	74 (1)	10 (1)	−16 (1)	−9 (1)
	−8779 (3)	24132 (3)	9905 (2)	68 (1)	74 (1)	79 (1)	10 (1)	−16 (1)	−9 (1)
S(2)	18488 (9)	9427 (9)	16256 (9)	52 (4)	64 (4)	68 (4)	11 (3)	−23 (3)	−10 (3)
	18500 (3)	9411 (3)	16248 (3)	63 (1)	65 (1)	77 (1)	11 (1)	−20 (1)	−8 (1)
	18496 (3)	9409 (3)	16247 (3)	76 (1)	77 (1)	80 (1)	12 (1)	−24 (1)	−10 (1)
C(1)	1757 (5)	3902 (5)	1186 (5)	155 (20)	34 (15)	176 (20)	−52 (14)	19 (16)	9 (14)
	1746 (2)	3891 (2)	1192 (2)	112 (7)	72 (6)	157 (8)	−24 (6)	1 (5)	−7 (4)
	1743 (2)	3892 (1)	1192 (1)	104 (4)	67 (3)	135 (5)	−24 (3)	−1 (3)	1 (3)
C(2)	574 (5)	2963 (5)	3265 (4)	116 (19)	127 (19)	81 (18)	4 (15)	−8 (14)	8 (14)
	572 (2)	2963 (2)	3266 (1)	120 (7)	183 (8)	65 (6)	22 (6)	−7 (5)	−14 (4)
	570 (1)	2960 (2)	3263 (1)	127 (4)	147 (5)	66 (3)	23 (4)	−17 (3)	−15 (3)
P	8313 (10)	25808 (10)	17869 (8)	49 (4)	46 (4)	46 (4)	1 (3)	−13 (3)	−2 (3)
	8302 (3)	25788 (3)	17861 (3)	55 (1)	58 (1)	53 (1)	2 (1)	−11 (1)	−6 (1)
	8300 (3)	25786 (3)	17862 (3)	60 (1)	60 (1)	54 (1)	2 (1)	−11 (1)	−5 (1)
H(1)	191 (5)	371 (5)	44 (4)						
	185 (2)	373 (2)	56 (3)						
	180 (4)	384 (4)	43 (5)						
H(2)	264 (5)	377 (5)	156 (5)						
	247 (4)	389 (2)	151 (2)						
	258 (6)	396 (5)	162 (5)						
H(3)	117 (6)	465 (6)	124 (5)						
	135 (3)	464 (4)	127 (2)						
	132 (7)	472 (7)	125 (6)						
H(4)	17 (7)	221 (5)	359 (4)						
	20 (4)	229 (4)	356 (3)						
	9 (8)	230 (10)	358 (6)						
H(5)	121 (5)	309 (5)	359 (3)						
	131 (4)	311 (3)	358 (3)						
	123 (7)	314 (10)	375 (7)						
H(6)	−4 (8)	354 (6)	335 (5)						
	5 (4)	359 (4)	337 (2)						
	−9 (6)	347 (6)	317 (6)						

conservatively used the s.u. of the population in further least-squares analysis. In cases where only one datum existed the s.u.'s calculated by the *HIPPO* program were used.

Data were recorded out to $\sin\theta/\lambda = 1.774$ Å^{-1}, and those with thorium core contribution were often significant at this low temperature. The LO data set extended from 0 to 0.976 Å^{-1} and 73% of the data were integrated with positive intensity, while the HO data set extended from 0.259 to 1.774 Å^{-1} and 45% of the reflections were integrated. In the current version of *HIPPO* weak reflections with a very small initial skewness are not integrated, and thus no negative intensities are present in the data set. The HO data set included some 3700 unique reflections below 0.976 Å^{-1}. We should emphasize that in this tetragonal crystal, with the collection method used, there is considerable data redundancy in the LO data set. Each unique reflection was measured on average 19 times. The average data based on multiple measurements were very reliable, since *SORTAV* could reject outliers. In some cases where reflections were measured only twice or, occasionally, four times, *SORTAV* could not choose between disparate reflections and calculated average intensities with very high

Table 3. *Selected geometric parameters from the LO synchrotron data refinement using the sealed-tube unit cell (Å, °)*

Th—S(1)	2.9102 (4)
Th—S(2)	2.8787 (4)
P—S(1)	2.0114 (5)
P—S(2)	2.0127 (5)
C(1)—P	1.802 (2)
C(2)—P	1.803 (2)
C(1)—H(1)	0.77 (5)
C(1)—H(2)	0.84 (4)
C(1)—H(3)	0.89 (4)
C(2)—H(4)	0.88 (4)
C(2)—H(5)	0.86 (4)
C(2)—H(6)	0.85 (4)
S(1)—Th—S(2)	69.60 (1)
S(1)—Th—S(1^{i})	132.86 (1)
S(1)—Th—S(2^{i})	79.54 (1)
S(1)—Th—S(1^{ii})	67.70 (1)
S(1)—Th—S(2^{ii})	137.20 (1)
S(1)—Th—S(1^{iii})	134.37 (1)
S(1)—Th—S(2^{iii})	78.25 (1)
S(2)—Th—S(2^{i})	96.98 (1)
S(2)—Th—S(2^{ii})	153.19 (1)
S(2)—Th—S(2^{iii})	89.20 (2)
Th—S(1)—P	89.02 (1)
Th—S(2)—P	89.89 (2)
S(1)—P—S(2)	110.38 (2)
S(1)—P—C(1)	110.50 (6)
S(1)—P—C(2)	109.58 (6)
S(2)—P—C(1)	108.96 (6)
S(2)—P—C(2)	110.85 (6)
C(1)—P—C(2)	106.50 (9)
H(1)—C(1)—P—C(2)	−179 (2)
H(2)—C(1)—P—C(2)	65 (2)
H(3)—C(1)—P—C(2)	−58 (2)
H(4)—C(2)—P—C(1)	174 (3)
H(5)—C(2)—P—C(1)	−54 (2)
H(6)—C(2)—P—C(1)	70 (3)

Symmetry codes: (i) $-x, -y, z$; (ii) $-y, -x, -z$; (iii) $y, x, -z$.

s.u.'s often ten times those of other reflections of comparable intensity. These were rejected on the grounds that one of the reflections was not measured correctly, for reasons outlined below. In addition, in the final refinements of both the LO and the HO data sets it was noted that *ca* 1% of the reflections were extreme outliers, with $(I_{obs} - I_{calc})/\sigma(I_{obs})$ between +10 and +140, with I_{calc} of low value, but which could not be eliminated on statistical grounds. These outliers remaining in the final data were almost invariably those few unique reflections measured only once, but in some instances two or three times, for which outliers are not statistically assignable. For the LO data set we have therefore discarded *all* reflections measured only once, together with *ca* 50 outliers measured two or three times. Those discarded were probably not integrated correctly. We observe that the integration program sometimes fetches neighbouring intensity due to inaccurate spot prediction and insufficently tight differentiation between neighbouring peaks. In addition there were a small number of reflections for which I_{obs} was unbelievably lower than I_{calc}. This can also be associated with inaccurate spot prediction in small regions. The HO data is less redundant (only 3843 data were measured three times or more) and so these data are less reliable on a reflection-by-reflection basis. In the HO data it is therefore more difficult to discriminate against extreme outliers before the final refinement, and these were discarded solely on the basis of a very poor fit to the multipole model, $[|\Delta F^2/\sigma(F^2_{obs})| > 10]$.† In Table 1 various internal R factors are listed. The abnormally large weighted R factors wR for the synchrotron data reflect the presence of weak outlier reflections in the data, which cannot be rejected on statistical grounds as discussed above. This shows that at the present stage of development of the synchrotron image-plate technique removal of gross outliers based on a structure model is critical for obtaining an accurate data set for ED analysis. The area-detector technique allows in general high redundancy even for synchrotron data because of the high data-collection rate. This is essential for realizing and discarding outliers. We cannot emphasize strongly enough the importance of high data redundancy for obtaining accurate data, particularly since the time penalty is small when using an image-plate system.

3. X-ray data modelling

The three separate sets of unique X-ray data (the sealed-tube, the HO and the LO synchrotron data sets) were refined using the *ASRED* program (Figgis *et al.*, 1980), in which the observations were fitted to a harmonic model of nuclear position and displacement and a multipole model of the ED described in more detail below. We also included simplified corrections for multiple scattering and type II extinction, a method described in more detail elsewhere (Figgis *et al.*, 1993). Since $h + k + l$ odd and $h + k + l$ even reflections are on average very different in intensity, due to the difference in thorium contributions, we may expect differences in multiple scattering, and therefore separate $h + k + l$ odd and $h + k + l$ even multiple-scattering parameters were refined. The quantity $\Sigma\{[F^2_{obs} - F^2_{calc}]^2/\sigma(F^2)^2\}$ was minimized until a maximum shift/s.u. of 0.1 was obtained.

The positional parameters of all 12 unique atoms were refined, starting from the values of the original structure determination and interpolated H-atom positions using known methyl-group geometry (Pinkerton *et al.*, 1981). We refined only isotropic harmonic displacement parameters for the H atoms, but anisotropic harmonic displacement parameters for the heavy atoms. Anom-

† Supplementary data for this paper are available from the IUCr electronic archives (Reference: LC0008). Services for accessing these data are described at the back of the journal.

alous-dispersion corrections were calculated for thorium and the other heavy atoms (Brennan & Cowan, 1992). We note that the calculated values for Ag radiation for thorium ($f' = -3.74$, $f'' = 9.89$ e) are substantially larger than for the synchrotron wavelength ($f' = -1.04$, $f'' = 5.64$ e).

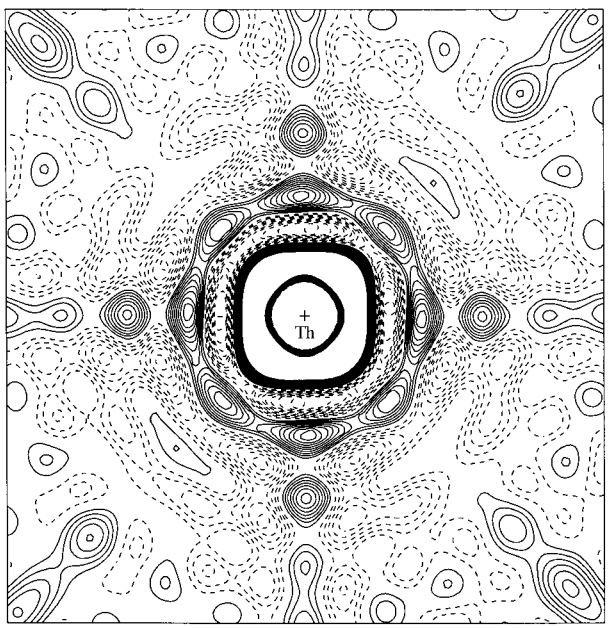

Fig. 2. The experimental deformation density around the Th site in the Th—S(1)—P plane. The contour interval is 0.1 e Å^{-3} and the resolution is 0.7 Å^{-1}. Both very low and high level contours are suppressed.

The valence model for the charge density consisted of atom-centred functions. Core electron-density functions on the heavy atoms and valence distributions on all atoms were obtained from a standard compilation (*International Tables for X-ray Crystallography*, 1974, Vol. IV) or by use of the program *JCALC* (Figgis *et al.*, 1987) with Hartree–Fock atomic wavefunctions (Clementi & Roetti, 1974). The valence functions on Th consisted of the difference of Th and Th^{4+} form factors, *i.e.* the $6d^2 7s^2$ form factor together with some core rearrangement, with angular variation up to fourth-order multipoles. In addition we added a more contracted set, arbitrarily chosen with Tc 4*d* radial dependence (Reynolds *et al.*, 1997), again with angular dependence up to fourth order. On S, P, and C centres, since molecular changes and atomic calculations are more reliable than for Th, less flexibility is required. We placed 3*p*, 3*p* and 2*p* radial dependence with angular variation to third order on S, P and C, respectively, and a spherical 1*s*-like distribution (Stewart *et al.*, 1965) on H. The radial extent of all the valence functions was allowed to vary in the usual κ refinement (Coppens *et al.*, 1979) and all valence populations were allowed to vary. Because of uncertainty in the relativistic treatment of the atomic calculation for such a heavy atom as thorium, the core radius was also allowed to vary in the κ manner. In addition Gaussian density of width 0.16 Å^2 was placed at the six independent bond midpoints between non-H atoms to help model bond overlap density, and the populations of these were refined. The total unit-cell contents were constrained to the formula number of electrons.

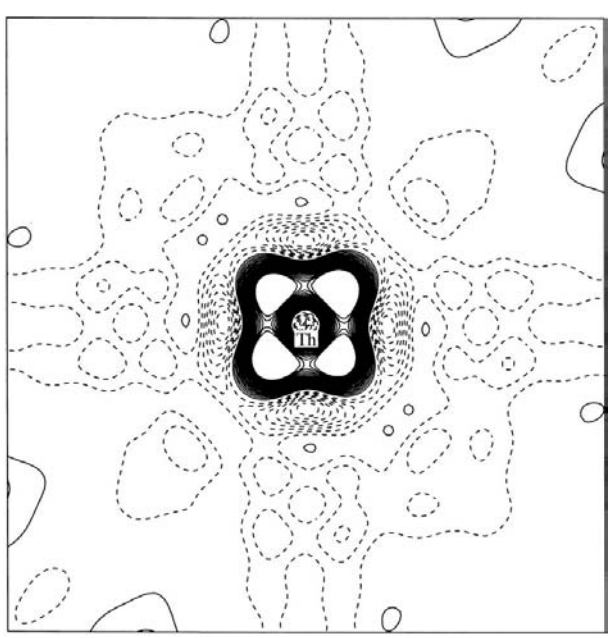

Fig. 3. Radially adjusted model deformation density in the (001) plane around the Th site. Contours as in Fig. 2.

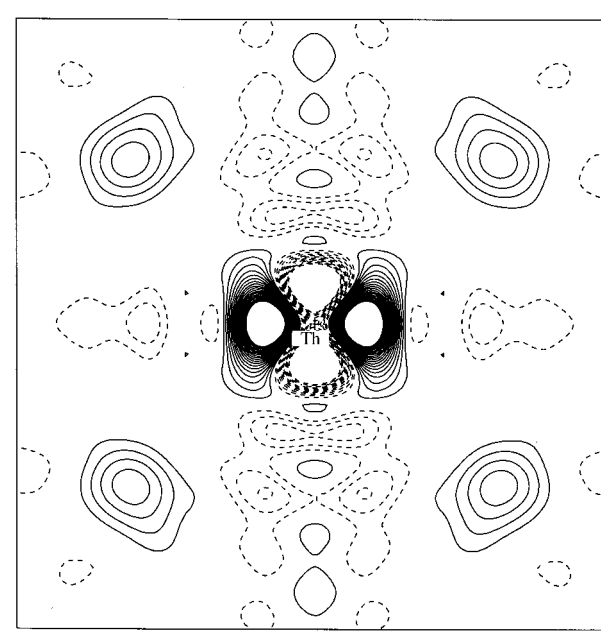

Fig. 4. Radially adjusted model deformation density in the (110) plane around the Th site. Contours as in Fig. 2.

Since the thorium atom is very heavy and contributes strongly to only half of the reflections ($h + k + l$ even), the intensities of which it tends to dominate, its charge becomes more uncertain than for other atom sites. The refined value of the thorium charge becomes dominated by the relative scale factors of $h + k + l$ even and $h + k + l$ odd reflection classes. This ratio in turn has systematic errors due to the different effects of multiple scattering in the strong $h + k + l$ even and weaker $h + k + l$ odd data, and the effect of extinction. Since Th^0 has 90 electrons, to define its charge to chemical accuracy requires knowledge of the scale factors and extinction corrections to better than 1%. We have therefore constrained the thorium charge to +1 in the sealed-tube data and HO synchrotron data sets, a value consistent with *ab initio* calculations (Iversen *et al.*, 1998) and general chemical expectations arising from Pauling's principle of electroneutrality. We should note that we later determine that this generally acceptable assumption may not in fact be correct! We find that the LO synchrotron data set contains enough low-angle data of sufficient accuracy to refine the Th-site total charge.

While the ligand densities in any model are defined quite well by the $h + k + l$ odd data alone, there are many aspherical components on the thorium site defined only by the $h + k + l$ even data. Of the d-type distributions only the difference of d_{xz} and d_{yz} are defined by the $h + k + l$ odd data; d_{z^2}, $d_{x^2-y^2}$, d_{xy} and ($d_{xz} + d_{yz}$) are all fixed by the $h + k + l$ even data. However, such anisotropic terms are much less affected than the total charge by scale-factor errors. This is because, in terms of the ratio of the error to the fitted values, useful chemical information is obtained with much poorer relative definition of the values. While in the refinement we notice that spherical (monopole) terms are only slightly correlated with aspherical (higher multipole) terms it is well known that an indirect connection can be observed through poor treatment of extinction and absorption. However, this is unlikely here since both are relatively isotropic and not large in size. Thus, ligand terms as well as aspherical terms on the thorium are well defined by this data.

The anomalous dispersion from the Th sites is large, so for the LO synchrotron data set and the sealed-tube data set we performed a refinement with both real and anomalous parts varying. As for the thorium-core scattering factor, there is some uncertainty in theoretical calculations of anomalous-scattering contributions for heavy atoms. The present data allow an independent experimental determination of these quantities. The anomalous dispersion remained at the calculated values, within 1σ, with errors in both of *ca* 0.4 e. In subsequent refinements these values were fixed at calculated values. Extinction effects in the refinements were small. For the synchrotron data 15 reflections had $y < 0.92$ with the minimum being 0.85. All these reflections are very well modelled by the model described above, showing that the isotropic extinction model is adequate in the present case. For the conventional data, extinction effects are negligible with $y_{min} = 0.99$.

Table 4. *Comparison of R(F) for refinement of reflections common to the sealed-tube and LO synchrotron data*

	$R(F)$ (tube)	$R(F)$ (LO)	No. of data
$0 < \|F\| < 50$	0.080	0.022	896
$50 < \|F\| < 100$	0.021	0.008	672
$100 < \|F\| < 150$	0.011	0.005	380
$150 < \|F\|$	0.014	0.008	37
All	0.026	0.009	1985

The agreement factors are listed in Table 1 for the three data sets, and derived positional and displacement parameters for the refinements are given in Table 2. The molecular geometry is given in Table 3 based on refinement of the LO synchrotron data. Fig. 1 shows the molecular geometry.

4. Separation of anharmonic and electron-deformation effects

Detailed discussion of the electronic structure and chemical bonding in the complex is provided in our companion paper where the experimental model ED is compared with *ab initio* theory (Iversen *et al.*, 1998). Here we present points which are specifically related to the fundamental question of separating thermal-motion effects from electron deformation. The experimental deformation density is calculated by subtracting from the observed ED that of a molecule composed of a superposition of free-atom densities. The observed density is estimated by using a Fourier summation of $|F_{obs}|$ with phases derived from the best model calculation. The residual density uses ($|F_{obs}| - |F_{model}|$) phased with model phases. Finally, the model deformation density is the difference between the experimental deformation and residual densities. If the model provides a good fit to the data and thus gives a low residual density, the model deformation density is ideally a noise-filtered version of the experimental deformation density. In the present case the two types of deformation densities are found to be dominated by the apparent radial change in core density on Th. Fig. 2 shows a typical section through the Th site and illustrates typical truncation errors giving oscillation in the deformation density. Since this is a spherical term centred on the Th site it is the least reliable effect and obscures other better estimated information (aspherical features on thorium and ligand information). Accordingly we have recalculated the promolecule density incorporating the 3.3 (5)% expansion modelled on the Th core in the Th atom density. In Figs. 3 and 4 radially adjusted model deformation densities are shown for two perpendicular sections through the Th atom [planes (001) and (110)]. The plots reveal a large anisotropic polarization on the Th site. Thus there is a substantial

Table 5. *Comparison of relative standard uncertainties for common sealed-tube and LO synchrotron data*

	$\Sigma\sigma(I)/\Sigma I$ (tube)	$\Sigma\sigma(I)/\Sigma I$ (LO)	No. of data
$0 < I < 0.0033I_{max}$	0.136	0.050	939
$0.0033I_{max} < I < 0.0166I_{max}$	0.044	0.021	648
$0.0166I_{max} < I < 0.0333I_{max}$	0.034	0.017	241
$0.0333I_{max} < I$	0.029	0.014	157
All	0.039	0.018	1985

depletion along [001] and accumulation along [110]. This redistribution of charge has been successfully modelled by the contracted *d* functions on the Th site with a 3.7 (3) e deficit in the $xz + yz$ orbitals, and an excess of 1.2 (2) e in xy and of 3.5 (2) e in $x^2 - y^2$ (compared to a spherical radon-like core). The chemical significance of this core polarization is discussed in our companion paper. Here we note that very large xy valence changes from Th^0 are observed.

The small thermal motion, essentially zero-point, at 28 (5) K is noticeable. The low atomic displacements and the lack of phase transitions or Jahn–Teller effects lead us to expect negligible anharmonic displacement parameters – although we should note that just as the zero-point motion has a harmonic component it may also sometimes have anharmonic components, particularly in cases involving hydrogen motion. We have tested this by a refinement using the HO synchrotron data set, which extends to 1.77 $Å^{-1}$, of third-order Gram–Charlier anharmonic parameters for all heavy atoms together with symmetry-adapted anisotropic fourth-order anharmonic parameters on the Th site. There was slight but hardly significant improvement considering that 52 extra parameters were included in the refinement. The goodness-of-fit decreased from 1.89 to 1.82 and $R(F)$ from 0.030 to 0.028, and only a single anharmonic parameter exceeded the 4σ level of significance. This was a fourth-order thorium parameter of the form $q_x^2 q_y^2$. Given the large xy valence changes from Th^0 observed in the valence refinement, we believe this parameter is partly accommodating residual bonding effects at higher angles. If the anharmonic parameters are fixed at values obtained in the HO data refinement and are used in refinement of the LO data, then the values of the valence functions, in particular the contracted *d* functions on the thorium, are hardly changed. Thus, we observe only a slight correlation between anharmonicity and electron deformation, and that the anharmonic parameters are ineffective in modelling of the xy deformation. In subsequent refinement of the LO data set we therefore only used harmonic displacement parameters.

Restori & Schwarzenbach (1996) have asserted that anharmonic and electron-deformation bonding effects are not practically separable when using X-ray data obtained at a single temperature. They show theoretically that if atoms are represented by Gaussian distributions and sufficiently flexible valence-electron representations are used then anharmonicity and valence deformation are completely correlated, and thus inseparable in a single data set. It is clear that a complete series expansion in reciprocal space ('anharmonicity') can always fit the same single data set identically to a complete enough electron-deformation-density expansion in real space. Thus definition of nuclear motion would appear to require neutron diffraction or several X-ray data sets at different temperatures. They illustrated this with the case of K_2PtCl_6, which at 100 K can be fitted either by electron-deformation functions or by anharmonic functions. However, to fit their 100 K K_2PtCl_6 data without invoking anharmonicity at all, Restori & Schwarzenbach require valence functions implying Slater exponents for the K site of 6.8 (15) $bohr^{-1}$. This is about equivalent to a valence polarization of K 2*s* orbitals (Clementi & Roetti, 1974), which seems physically unlikely.

In the present case we are better placed to separate deformation and anharmonicity. Our data extend 30% further in $(\sin\theta/\lambda)^2$ than the K_2PtCl_6 data, while the thorium mean-square displacement is only half that for Pt, and all motions are essentially zero-point. Given that the core densities for both Th and Pt are far from Gaussian, these factors make our contracted *d* function on Th and our set of anharmonic parameters only slightly correlated experimentally, and thus separable using the full extent of our data. However, in agreement with Restori & Schwarzenbach's conclusions, if we restrict the maximum $\sin\theta/\lambda$ to, for example, 0.95 $Å^{-1}$, the correlation between our contracted *d* functions and the anharmonic parameters is almost complete. If we included anharmonic parameters of even higher order than four then, no doubt, we could fit all the data without contracted *d* functions, but this seems physically unreasonable. In addition, the values of the anharmonic parameters required to fit the restricted data, without contracted *d* functions, are a factor of 10–20 times larger than the values refined from the full data set. These values are much larger than expected for zero-point values in a vibrationally well behaved crystal.

Thus for data which are extended in reciprocal space and are measured at very low temperatures, and if neither unrealistic very high order anharmonicity nor electron polarization deep into the core is used, then valence deformation and anharmonicity are in practice separable. However, in cases where the anharmonicity may be larger both absolutely and relative to harmonic

motion, such as with typical room-temperature data, or where there is instability of crystal phase or of the Jahn–Teller type, good neutron data will indeed be required to convincingly separate anharmonicity and electron-polarization effects.

5. Results and discussion

The great advantage of the synchrotron experiment over the sealed-tube data is the data-collection speed. We obtained 20 times as much data in one-seventh of the time. However, sealed-tube data, when properly collected, are of good and consistent quality. In contrast to this, many synchrotron data sets have often been of inferior quality, with only few studies achieving results comparable to the best sealed-tube data. For good-quality data we should often expect $R(F^2)$ of about 0.02 and $R(F)$ of 0.01 for small-molecule structures. Furthermore, the few synchrotron-radiation studies which have achieved a quality comparable to high-quality sealed-tube data (Kirfel & Eichhorn, 1990) were all carried out on very small unit cell inorganic structures of high symmetry with only a few thousand reflections collected. To our knowledge the present study is the first in which a very large number of accurate data has been collected on a compound of general chemical interest using a synchrotron source. The term accurate is again in this context implying very low temperature data. As mentioned above, we have previously shown that data measured at liquid-nitrogen temperatures in general contain considerable systematic errors and are significantly less useful for ED modelling.

To assist in comparing the quality of the data sets we have refined a subset of the LO synchrotron data and the sealed-tube data in which we have used reflections common for the two data sets. There are 2529 sealed-tube data, but only 2098 synchrotron data in the same region of reciprocal space. Of these reflections there are 1985 in common, *i.e.* 113 reflections are present in the synchrotron LO data but not in the sealed-tube data, and 644 reflections are in the sealed-tube data but not in the synchrotron LO data. This difference is primarily due to the processing of the synchrotron data, which has failed to integrate certain peaks satisfactorily, and secondly due to very weak data only being significant with intense synchrotron radiation. The missing synchrotron data relative to the sealed-tube data are mostly found for $\sin\theta/\lambda > 0.5$ Å^{-1}. Below 0.5 Å^{-1} the synchrotron data are more complete than the sealed-tube data, except in the very low order region in which only five out of 18 reflections with $\sin\theta/\lambda < 0.15$ Å^{-1} are present in the synchrotron data. Very low order data are difficult to integrate in the present experimental setup when very short wavelengths are used. In Tables 4 and 5 values of $R(F)$ and $\Sigma\sigma(I)/\Sigma I$ are shown for various subsections of the common data. Several points are worth noting from the direct comparison. First of all it is clear that the synchrotron data are better for all classes of reflections, but particularly superior for weak reflections. The present study deals with a large number of very weak reflections and this makes the synchrotron data collection especially rewarding. Table 4 reveals that the synchrotron data give unusually low R factors even for very weak reflections. At the same time the synchrotron data also have a much better overall precision with considerably smaller relative uncertainties. The results therefore indicate that the synchrotron data at lower angles are superior to the sealed-tube data. It is not possible to compare the two sets of $|F_{obs}|^2$ directly since both the temperature and extinction are different. Even at these low temperatures, where the temperature dependence is small, we may expect differences in displacement parameters of a few Å^2 $\times$ 10^{-4}, which translate into intensity changes of a few per cent for the higher-angle sealed-tube data (*ca* 1 Å^{-1}).

The direct comparison of common reflections does not give the full picture of the present status of the two data-collection methods. The fact that we get different data sets in a given region of reciprocal space is important. Even though the sealed-tube data collection is slower and less accurate than the synchrotron data collection, it still potentially measures everything. The synchrotron data are superior for weak reflections and extend very far in reciprocal space, but sometimes contain completely wrong intensities. This makes redundancy imperative for obtaining accurate synchrotron data. Furthermore, lack of very low angle data potentially adds uncertainty, for example when defining atomic charges in a multipole refinement, although in the present study only the LO synchrotron data were able to define the Th charge to chemical accuracy. If we refine the model using the 2098 LO synchrotron reflections found in the same region of reciprocal space as the sealed-tube data we obtain goodness-of-fit 0.82, $R(F^2)$ (all data) 0.013, $wR(F^2)$ (all data) 0.019 and $R(F)$ 0.0087 for the 2007 reflections with $F^2 > 3\sigma(F^2)$. Both the agreement factors and the parameter s.u.'s are noticeably lower for the synchrotron data. This reflects both the loss of unintegrated weak data and better counting statistics in the weak data that are found. Where the weak synchrotron data have been successfully integrated the resulting s.u.'s are clearly superior. This can be seen in the agreement factor $R(F)$ being far superior for the synchrotron data, but $R(F^2)$ still being better, but with a lesser margin. $R(F)$ is of course more weighted towards weaker reflections than $R(F^2)$. The refined values of the parameters obtained from the synchrotron data do not change markedly on restriction of the data set, although the s.u.'s do inflate a little.

In the present case the synchrotron data appear to be more consistent than the sealed-tube data. We note that the repeated measurement of reflections has apparently overcome the worse internal agreement factor for the synchrotron data, again emphasizing the value of

redundant measurements. The overall agreement factors for the LO synchrotron data set are acceptable, *e.g.* we obtain an $R(F)$ of 0.011. The sealed-tube data-agreement factors are marginally higher than is normally obtained from this instrument. We attribute this mostly to the large intensity loss in the standards and necessary renormalization of the data. The intensity loss was presumably caused by crystal degradation. Indeed, it was observed that the crystal had turned opaque at the end of the sealed-tube measurements. This shows another advantage of the short data-collection time at the synchrotron source. It should also be noted that absorption remains high even at the Ag $K\alpha$ wavelength. The higher agreement factors for the HO synchrotron data are partly the unavoidable result of measuring much $h + k + l$ odd data which are very weak, and partly the result of insufficient multiple measurements of reflections.

To obtain some estimate of systematic errors, rather than the random errors dealt with above, we compare the values of the derived positional and displacement parameters in Table 2. The positional parameters among the three parameter sets agree within two standard uncertainties for the non-H atoms and three standard uncertainties for the H atoms. We note that the LO synchrotron data give s.u.'s smaller than the sealed-tube data by a factor of two or three, reflecting both the better agreement and more extensive data. However, the greater extent and number of data in the HO synchrotron data set are only just sufficient for the non-H atoms to make up for the poorer agreement between model and experiment. At the two experimental temperatures the thermal motion is essentially zero-point and temperature-independent, although at 28 K we may expect an increase of a few $\text{Å}^2 \times 10^{-4}$ in the displacement parameters over those at 9 K, given typical Debye temperatures for this type of organometallic material. While the off-diagonal elements and anisotropy in the diagonal elements of the displacement parameters agree well, there are larger than expected systematic differences in the trace of the displacement tensors. The Th displacement parameters agree well for the HO and the LO synchrotron data, but for the other non-H atoms there is a mean difference of 9×10^{-4} Å^2 in the trace. In comparing the sealed-tube and LO synchrotron data for the Th atom there is a -20×10^{-4} Å^2 difference, while the difference is 9×10^{-4} Å^2 for the other non-H atoms. These differences are small in absolute terms owing to the very low temperatures of the experiments. Since the large relative difference for Th is not carried through for the other non-H atoms, it may not be caused by remaining θ-dependent systematic errors. The differences in the present study are larger than the *ca* 3×10^{-4} Å^2 differences observed between X-ray and independent neutron diffraction results involving both time-of-flight and reactor data in other recent cases involving this apparatus (Figgis *et al.*, 1993; Iversen *et al.*, 1996). However, it should be remembered that the sealed-tube data in this study are of slightly lesser quality than normal for this instrument due to the crystal decay. Overall the comparison suggests that a small systematic error remains in the synchrotron data, which should probably not be relied on to better than 10×10^{-4} Å^2 in absolute assessment of displacement parameters. This is still a very satisfactory result. Iversen *et al.* (1996) examined displacement parameters for a number of combined X-ray and neutron studies. At liquid-nitrogen temperatures typical discrepancies between X-ray and neutron data are 20×10^{-4} Å^2 or more, even for small organic structures. Clearly the very low temperature synchrotron data are superior to such studies even at the present stage of development of the technique.

The fact that consistent displacement parameters can be obtained from the synchrotron data is important for the deconvolution of the thermal motion from the X-ray data to obtain static ED distributions. Static EDs can be directly compared with results of theoretical calculations or analysed with topological methods (Bader, 1990). It may be argued that if the systematic errors in the data are absorbed solely in the displacement parameters then the deconvolution is still correct. This is however not the case as shown by Iversen *et al.* (1997) for $Ni(ND_3)_4(NO_2)_2$.

6. Conclusion

The present study shows that synchrotron data collected at very low temperatures have now reached a stage where they are comparable to the best conventional data. Use of area detectors allows data to be collected in a matter of days, greatly increasing the scope of experimental ED studies. We cannot emphasize strongly enough the need for data redundancy when measuring image-plate data, especially because the time penalty is small. Comparison of structural parameters derived separately from conventional and synchrotron data shows good agreement, but the study suggests that small systematic errors still exist in the synchrotron data. Presently, displacement parameters derived from very low temperature image-plate synchrotron data should not be relied on to better than 10×10^{-4} Å^2. This error is, however, small in absolute terms, and smaller than typical systematic errors encountered in data measured at liquid-nitrogen temperatures. The present study is the first accurate area-detector synchrotron-radiation study, and the results show that ED studies of compounds of general chemical interest can now be carried out. For studies of heavy-metal complexes, where demands for accuracy are high, it is crucial to cool to the lowest possible temperature to obtain reliable data. Finally, we have shown that it is possible to separate anharmonic effects from electron-deformation effects even for a single temperature X-ray data set, provided very low

temperature data extending far in reciprocal space are available.

BBI and FKL gratefully acknowledge support from the Carlsberg Foundation and a DANSYNC grant from the Danish Natural Science Research Foundation. The research was carried out in part at the National Synchrotron Light Source at Brookhaven National Laboratory, which is supported by the US Department of Energy, Division of Materials Sciences and Division of Chemical Sciences. The SUNY X3 beamline at NSLS is supported by the Division of Basic Energy Sciences of the US Department of Energy (DEFG0286ER45231).

References

Bader, R. F. W. (1990). *Atoms in Molecules. A Quantum Theory.* Oxford: Clarendon Press.

Blessing, R. H. (1989). *J. Appl. Cryst.* **22**, 396–397.

Bolotovsky, R. & Coppens, P. (1997). *J. Appl. Cryst.* **30**, 65–70.

Bolotovsky, R., Darovsky, A., Kezerashvili, V. & Coppens, P. (1995). *J. Synchrotron Rad.* **2**, 181–184.

Bolotovsky, R., White, A. M., Darovsky, A. & Coppens, P. (1995). *J. Appl. Cryst.* **28**, 86–95.

Brennan, S. & Cowan, P. L. (1992). *Rev. Sci. Instrum.* **63**, 850–853.

Burnett, M. N. & Johnson, C. K. (1996). *ORTEP*III. Report ORNL-6895. Oak Ridge National Laboratory, Tennessee, USA.

Chandler, G. S., Figgis, B. N., Reynolds, P. A. & Wolff, S. K. (1994). *Chem. Phys. Lett.* **225**, 421–426.

Clementi, E. & Roetti, C. (1974). *At. Data Nucl. Data Tables*, **14**, 177–478.

Coppens, P. (1974). *DATAP.* Department of Chemistry, State University of New York at Buffalo, Buffalo, NY 14214, USA.

Coppens, P. (1992). *Synchrotron Radiation in Crystallography.* New York: Academic Press.

Coppens, P., Guru Row, T. N., Leung, P., Stevens, E. D., Becker, P. J. & Yang, Y. W. (1979). *Acta Cryst.* A**35**, 63–72.

Darovsky, A. (1995). Private communication.

Darovsky, A., Bolotovsky, R. & Coppens, P. (1994). *J. Appl. Cryst.* **27**, 1039–1040.

Darovsky, A. & Kezerashvili, V. (1997). *J. Appl. Cryst.* **30**, 128–132.

Darovsky, A., Meshkovsky, I. & Coppens, P. (1995). *J. Synchrotron Rad.* **2**, 77–78.

DeTitta, G. T. (1985). *J. Appl. Cryst.* **18**, 75–79.

Figgis, B. N., Iversen, B. B., Larsen, F. K. & Reynolds, P. A. (1993). *Acta Cryst.* B**49**, 794–806.

Figgis, B. N., Khor, L., Kucharski, E. S. & Reynolds, P. A. (1992). *Acta Cryst.* B**48**, 144–151.

Figgis, B. N., Reynolds, P. A. & White, A. H. (1987). *J. Chem. Soc. Dalton Trans.* pp. 1737–1745.

Figgis, B. N., Reynolds, P. A. & Williams, G. A. (1980). *J. Chem. Soc. Dalton Trans.* pp. 2339–2347.

Henriksen, K., Larsen, F. K. & Rasmussen, S. E. (1986). *J. Appl. Cryst.* **19**, 390–394.

Iversen, B. B. (1997). *Correction.* University of Aarhus, DK-8000 Aarhus C, Denmark.

Iversen, B. B., Larsen, F. K., Figgis, B. N. & Reynolds, P. A. (1997). *J. Chem. Soc. Dalton Trans.* pp. 2227–2240.

Iversen, B. B., Larsen, F. K., Figgis, B. N., Reynolds, P. A. & Schultz, A. J. (1996). *Acta Cryst.* B**52**, 923–931.

Iversen, B. B., Larsen, F. K., Pinkerton, A. A., Martin, A., Darovsky, A. & Reynolds, P. A. (1998). *Inorg. Chem.* **37**, 4559–4566.

Iversen, B. B., Nielsen, S. K. & Larsen, F. K. (1995). *Philos. Mag. A*, **72**, 1357–1380.

Kirfel, A. & Eichhorn, K. (1990). *Acta Cryst.* A**46**, 271–284.

Koritzansky, T., Flaig, R., Zobel, D., Krane, H.-G., Morgenroth, W. & Luger, P. (1998). *Science*, **279**, 356–358.

Larsen, F. K. (1995). *Acta Cryst.* B**51**, 468–482.

Lehmann, M. S. & Larsen, F. K. (1974). *Acta Cryst.* A**30**, 580–584.

Nielsen, F. S., Lee, P. & Coppens, P. (1986). *Acta Cryst.* B**42**, 359–364.

Pinkerton, A. A., Storey, A. E. & Zellweger, J.-M. (1981). *J. Chem. Soc. Dalton Trans.* pp. 1475–1480.

Restori, R. & Schwarzenbach, D. (1996). *Acta Cryst.* A**52**, 369–378.

Reynolds, P. A., Figgis, B. N., Forsyth, J. B. & Tasset, F. (1997). *J. Chem. Soc. Dalton Trans.* pp. 1447–1453.

Schultz, T. (1998). PhD thesis, University of Aarhus, DK-8000 Aarhus C, Denmark.

Stevens, E. D. & Coppens, P. (1976). *Acta Cryst.* A**32**, 915–917.

Stewart, R. F., Davidson, E. R. & Simpson, W. T. (1965). *J. Chem. Phys.* **42**, 3175–3187.

Zaleski, J., Wu, G. & Coppens, P. (1998). *J. Appl. Cryst.* **31**, 302–304.